Computation of Sound Radiation in an Axisymmetric Supersonic Jet

Yong Seok Kim*

Korea Automotive Technology Istitute
74 Yongjung-Ri, Pungse-Myun, Chonan, Chungnam, 330-912, KOREA

Duck Joo Lee**

Division of Aerospace Engineering, Department of Mechanical Engineering
Korea Advanced Institute of Science and Technology
373-1 Kusong-Dong, Yusung-Gu, Taejon, 305-701, KOREA

Abstract

An axisymmetric supersonic jet is simulated at a Mach number 2.1 and a Reynolds number of 70000 to identify the mechanism of Mach wave generation and radiation from the jet. In order to provide the near-field radiated sound directly and resolve the large-scale vortices highly, high-resolution essentially non-oscillatory(ENO) scheme, which is one of the Computational AeroAcoustics(CAA) techniques, is newly employed. Perfectly expanded supersonic jet is selected as a target to see pure shear layer growth and Mach wave radiation without effect of change in jet cross section due to expansion or shock wave generated at nozzle exit. The sound field is highly directional and dominated by Mach waves generated near the end of potential core. The near field sound pressure levels as well as the aerodynamic properties of the jet, such as mean-flow parameters are in fare agreement with experimental data.

Introduction

Jet is one of the fundamental fluid flows, the characteristic properties of which are well known. A good example of high speed jet flows is the exhaust flow from a jet engine which emits much annoying noise and undesirable gas components leading to air pollution. Moreover, reduction of supersonic jet noise plays a key role in operation of high-speed civil transports and rocket. Most high-speed jet accompanying propulsion systems produces intense radiated jet noise. The reduction of radiated noise is desired to minimize energy loss in the form of pressure wave. In rare cases, the acoustic waves can cause structural failure of the propulsion system by resonant interference with the structure. Thus, a good understanding of acoustic sources and the mechanism of sound radiation are very important.

Tam[1-3] gives a very extensive survey of the supersonic jet noise. According to his survey, it turns out that the noise characteristics of supersonic jets are quite complex and are very different from those of subsonic jets. It is now generally accepted that turbulent jet flows contain both fine-and large-scale turbulence structures. The relative importance of the noise they produce, however, depends to a large extent on the jet Mach number. The dominant part of subsonic jet noise is produced by the fine-scale turbulence. On the other hand, for supersonic jets, the large-scale vortices propagate downstream at supersonic Mach number relative to the ambient sound speed. As a result, they are capable of producing intense Mach wave radiation. Many

* Senior Researcher
  E-mail : yskim@katech.re.kr,   Tel : 041-559-3098,   Fax : 041-559-3091
** Professor

researchers[4-7] focused on the behavior of large-scale vortex produced in jet shear layer. Furthermore there is much concern with the relation between the spatial development of jet shear and the sound radiation from it. The identification of the large-scale coherent structure as a major sound source has been one of the most promising advances in the study of high-speed jet noise[8].

In this study, perfectly expanded supersonic axisymmetric jet issuing into a quiescent ambient environment is focused. It has been observed experimentally and numerically that the acoustic radiation from such jets is dominated by Mach waves[5,6,9,10]. We are interested in the mechanism of sound generation from a jet flow and near radiation field. That is, we would like to know the Mach wave generation and radiation due to the supersonic convection of large-scale vorticies.

Recently computer simulations have much been progressed along with visualization techniques and computing power. Several approaches are commonly used to solve the Navier-Stokes equations. The first one, the Direct Numerical Simulation(DNS), consists in calculating all turbulent scales. Mitchell et al.[11] performed DNS of both the near-field flow and far-field sound radiated from subsonic and supersonic axisymmetric jet. And Freund et al.[12-13] performed 3D DNS to investigate the noise radiated by supersonic and subsonic round jets. Nevertheless, DNS is restricted to low Reynolds numbers, and turbulence modeling is necessary to simulate higher Reynolds number flows characterized by a wider range of scales. One remedy for this is Large Eddy Simulation(LES)[14-16]. Only larger scales are calculated whereas the effects of smaller ones are assigned to a sub-grid scale model. However, 3D LES is also still expensive.

In the present study, numerical investigation of an axisymmetric supersonic jet is performed at a Mach number 2.1 and a Reynolds number of 70000. We do not employ a turbulence model because we are interested in the flow in the transitional region of jet, where disturbances grow in the shear layer. Mitchell et al.[11] mentioned that axisymmetric jets differ from fully turbulent jets, nevertheless, it is hoped that useful physical insights can be acquired. The purpose of this paper is to identify the mechanism of Mach wave generation and radiation from the jet using newly adopted ENO schemes and to validate both aerodynamic flow properties and near-field radiated sound by comparison with experimental data.

Numerical Algorithm

Governing equations and numerical scheme

The conservative forms of unsteady compressible axisymmetric Navier-Stokes equations in generalized coordinates are considered as follows:

$$\frac{\partial \hat{Q}}{\partial t} + \frac{\partial \hat{F}}{\partial \xi} + \frac{\partial \hat{G}}{\partial \eta} + \hat{H} = \frac{1}{\mathrm{Re}}\left(\frac{\partial \hat{F}_{\upsilon}}{\partial \xi} + \frac{\partial \hat{G}_{\upsilon}}{\partial \eta} + \hat{H}_{\upsilon}\right) \tag{1}$$

where

$$\hat{Q} = \frac{1}{J}\begin{vmatrix} \rho \\ \rho u \\ \rho v \\ \rho e_t \end{vmatrix}, \hat{F} = \frac{1}{J}\begin{vmatrix} \rho U \\ \rho u U + p\xi_x \\ \rho v U + p\xi_r \\ (\rho e_t + p)U \end{vmatrix}, \hat{G} = \frac{1}{J}\begin{vmatrix} \rho V \\ \rho u V + p\eta_x \\ \rho v V + p\eta_r \\ (\rho e_t + p)V \end{vmatrix}, \hat{H} = \frac{1}{J}\frac{1}{r}\begin{vmatrix} \rho v \\ \rho u v \\ \rho v^2 \\ (\rho e_t + p)v \end{vmatrix},$$

$$\hat{F}_{\upsilon} = \frac{1}{J}[\xi_x F_{\upsilon} + \xi_r G_{\upsilon}], \quad \hat{G}_{\upsilon} = \frac{1}{J}[\eta_x F_{\upsilon} + \eta_r G_{\upsilon}], \quad \hat{H}_{\upsilon} = \frac{H_{\upsilon}}{J} \tag{2}$$

The variables $\rho, u, v, p,$ and e_t are the density, two velocity components, pressure and total energy, respectively. And p is related to other variables by $p = \rho(\gamma - 1)\left[e_t - (u^2 + v^2)/2\right]$ where γ is the ratio of specific heat. $\hat{F}_v, \hat{G}_v, \hat{H}_v$ are related to viscous diffusion terms and are expressed in detail in the reference[17]. U and V are contravariant velocity components of the x, r directions respectively. The viscosity coefficient is assumed to be a function of temperature that was calculated by Sutherland's formula.

In this study we discretize the Navier-Stokes equations by the finite volume method with a spatially high accuracy modified flux approach ENO (essentially non-oscillatory) scheme[18-20] in order to solve the equations with sufficient accuracy and find the source of noise radiation. Regarding time integration, the Strang-type dimensional splitting was employed.

Computational domain and boundary conditions

The computational domain is shown schematically in Fig. 1. The computational domain includes the region $0 \le x \le 80D$ and $0 \le r \le 24D$, where D is a nozzle exit diameter, x is theaxial coordinate and r is the radial coordinate. Only the region $0 \le x \le 24D$ is considered to contain physically meaningful data since the region $24D \le x \le 80D$ is an exit zone constructedto allow large-scale vortices to exit the computational domain without reflecting significant disturbances back into the region of interest. The computational mesh had 860×400 points in axial and radial

Fig. 1. Schematic diagram of the computational domain. Note that the sketch is not to scale

directions respectively in physical domain, and 120×400 points in exit zone. Mesh points- were compressed in the radial direction near $r = R$, where R is the nozzle radius, and in the axial direction near the end of potential core x=8D.

Boundary conditions are crucial for long time noise calculation. Tam[21] summarized rigorously numerical boundary conditions for Computational AeroAcoustics(CAA). Thompson[22-23] and Poinsat and Lele[24]proposed to treat the problem as one-dimensional near the boundary of the computational domain. In this study, Thompson's characteristics-based boundary condition was used as nonreflecting boundary conditions at the inflow, outflow and top boundary. Based on the Thompson's approach, physical boundary conditions for the computation are derived by using characteristic variables w_i at ξ =constant boundary.
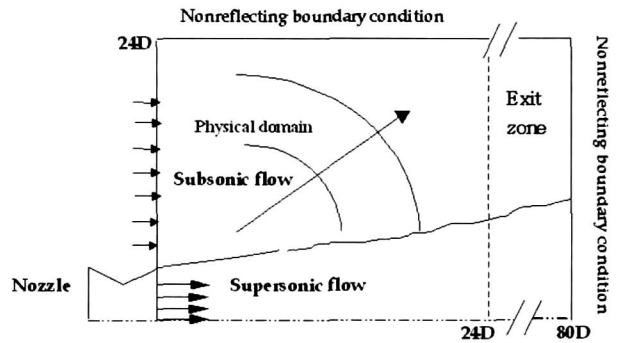
$$\delta w_1 = \delta\rho - \delta p / c^2$$
$$\delta w_2 = \delta\widetilde{V}$$
$$\delta w_3 = \rho c / \delta p + \delta\widetilde{U}$$
$$\delta w_4 = \rho c / \delta p - \delta\widetilde{U}$$

$$(3)$$

where c is the speed of sound and normal velocity's differentials are given as

$$\delta \widetilde{U} = \widetilde{\xi}_x \delta u + \widetilde{\xi}_r \delta v, \quad (\widetilde{\xi}_x, \widetilde{\xi}_r) = 1 \Big/ \sqrt{\xi_x^2 + \xi_r^2} \, (\xi_x + \xi_r) \tag{4}$$

And the velocity differentials in the direction parallel to the boundary surface are given as

$$\delta \widetilde{V} = -\widetilde{\xi}_x \delta v + \widetilde{\xi}_r \delta u \tag{5}$$

If one defines the relations between the amplitudes of characteristic waves L_i and characteristic velocities as

$$L_1 = u \left(\frac{\partial \rho}{\partial \xi} - \frac{1}{c^2} \frac{\partial p}{\partial \xi} \right)$$

$$L_2 = u \left(\frac{\partial \widetilde{V}}{\partial \xi} \right)$$

$$L_3 = (u + c) \left(\frac{1}{\rho c} \frac{\partial \rho}{\partial \xi} + \frac{\partial \widetilde{U}}{\partial \xi} \right)$$

$$L_4 = (u - c) \left(\frac{1}{\rho c} \frac{\partial \rho}{\partial \xi} - \frac{\partial \widetilde{U}}{\partial \xi} \right) \tag{6}$$

At each point on the boundary, the local one-dimensional inviscid(LODI) system is represented as follows

$$\frac{\partial \rho}{\partial t} + L_1 + \frac{\rho}{2c}(L_3 + L_4) = 0$$

$$\frac{\partial p}{\partial t} + \frac{\rho c}{2}(L_3 + L_4) = 0$$

$$\frac{\partial \widetilde{V}}{\partial t} + L_2 = 0$$

$$\frac{\partial \widetilde{U}}{\partial t} + \frac{1}{2}(L_3 - L_4) = 0 \tag{7}$$

At a supersonic inflow, all data are given, so that all time variations of the characteristic variables are set to zero, since all waves are incoming waves. At a supersonic outflow, all data can be obtained from the interior domain, so that all time variations of the characteristic variables are calculated using Eq. (7). Imposing a nonreflective subsonic inflow will consist in setting to zero the time variation of all incoming waves. In other words, L_4 is calculated as in Eq. (6) while all other δw_i are set to zero. The Eq. (6) and Eq. (7) allow us to impose certain inflow profiles. For present simulation, u velocity and density profiles were imposed through following relations;

$$L_3 = L_4$$

$$L_1 = -\frac{\rho}{c} L_4 \tag{8}$$

Because the jet exit condition is not known clearly it is necessary to estimate approximate nozzle exit conditions for use in the computations. The axial velocity component, u, by which the enters the computational region through the inflow boundary from its outside, should be given. In the present study, a curve fit for the velocity profiles that is obtained from Troutt et al.'s experiment[9] is applied. It takes the form of a half-Gaussian

$$u(r) = U_e \begin{cases} \exp[-2.773(\eta + 0.5)^2] & \text{for} \quad \eta > -0.5 \\ 1 & \text{for} \quad \eta \leq -0.5 \end{cases} \tag{9}$$

where $\eta = (r - r(0.5))/\delta$, and $u(r)$ represents a radial distribution of the axial velocity at the nozzle exit for the boundary condition. U_c is the velocity at the centerline of jet and r is the nozzle radius, i.e. $r = D/2$, $r(0.5)$ is the radial location where the velocity is 0.5 U_c. And δ is the local shear layer thickness. For the present calculation, $\delta/D = 0.04$ that is obtained from experimental data is used. The temperature profile by the Crocco-Busemann relationship is used to impose the density profile at the inflow boundary as follows:

$$T(r)/T_e = T_\infty/T_e + (1 - T_\infty/T_e)u(r)/U_c + (\gamma - 1)M_c^2 u(r)/U_c(1 - u(r)/U_c)/2 \tag{10}$$

where T_e represents the nozzle exit temperature and T_∞ represents ambient chamber temperature. At the inflow boundary, the radial velocity component V is set to zero. Inlet temperature is set to room temperature(294 K) and for the simulation of the perfectly expanded supersonic jet, inlet pressure is given to ambient chamber pressure.

Numerical Simulation Results

Pressure and vorticity distributions

Here in this study we numerically simulated an axisymmetric supersonic jet at a M=2.1 and at Re=70000. Because supersonic jet flow is highly unsteady, it is very difficult to determine the criterion of the stationary state. For this study, the stationary state numerical solutions are obtained when the mean axial and radial Mach number profiles are not changed as time goes on.

Mach waves, a dominant source of supersonic jet noise, are generated because large-scale eddies in the jet propagate with a convective velocity,

Fig. 2. Mach wave radiation due to a supersonic convection of eddies

which is supersonic with respect to the speed of sound, as shown Fig. 2. Discernible Mach waves are shown in pressure contour of Fig. 3. In general the pressure takes a low value at the location of vortex. Along the jet axis, the pressure takes high and low values alternatively
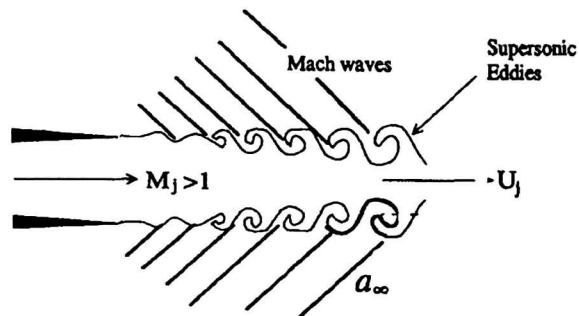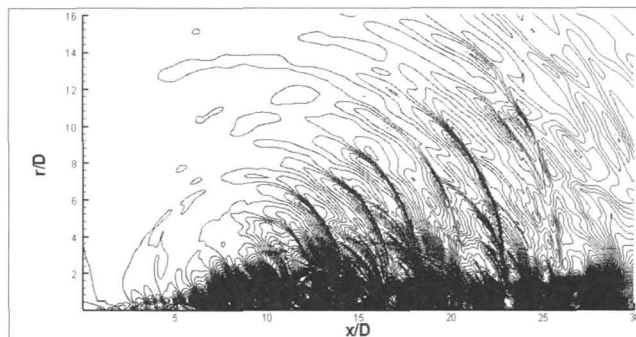
Fig. 3. Instantaneous contours of pressure: This figure shows Mach wave propagation until x / D=30
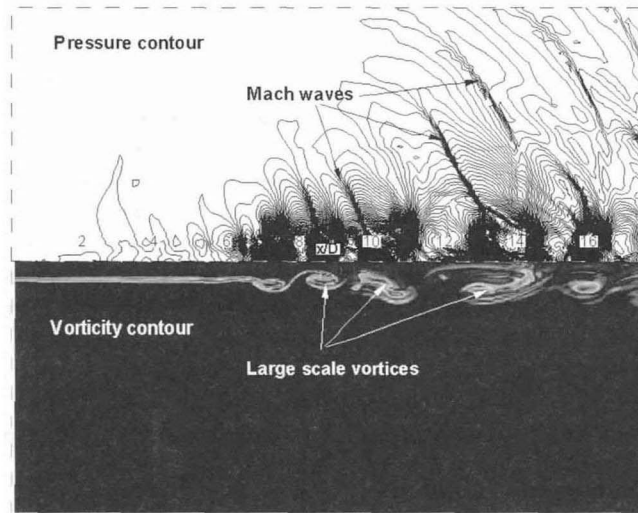
Fig. 4. Instantaneous contours of pressure and vorticity(zoomed view) : This figure shows Mach wave and Large scale vortices propagation until x / D=16
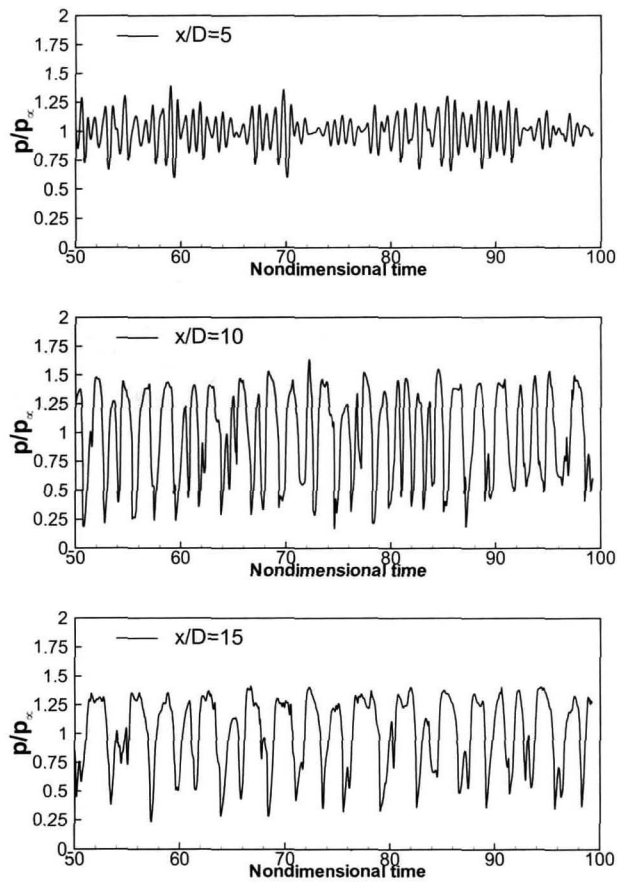

Fig. 5. Instantaneous pressure distribution along the shear layer(y=0.5D)

toward the downstream, which corresponds to each vortex location. This feature is shown as the instantaneous pressure distribution along the shear layer in Fig. 4.

On the other hand, between these vortices the pressure takes a large value, for example at $x/D \approx 8$, an adjacent vortex on its downstream side is pushed downstream. The axial width of this high pressure region becomes larger as we go downstream. It is found from the present simulation that as a result supersonic convection of these vortices in the downstream direction, intense pressure waves are produced outside the jet. The sound field is highly directional and sound appears to emanate primarily from the vicinity of the end of potential core($x/D \approx 8$) in Fig. 4 and Fig. 5, respectively. From the present simulation, location of the potential core end of the jet is approximately between 8 and 10 diameters as shown in vorticity contour of Fig. 4. This is similar that of Troutt's experiments[9]. At this region flow transitions to the turbulent are occurredin the shear layers. As shown in vorticity contour, vortex shapes of supersonic flow are flat and thin, while in subsonic flow this vortex takes a thick and round shape. This flattening of vortex is characteristic of high-speed shear layer.

Density and Mach number distributions

In Fig. 6, density contours are shown. Basically the density contours take almost the same shape as the pressure contours except a part of jet between vortices further downstream. In supersonic flows the Mach number is an important parameter to see the effect of compressibility. In Fig. 6, Mach number contours are shown, where the local Mach number is basically increased inside each vortex ring. Likewise pressure contours, the Mach waves are clearly shown in Mach number contours.
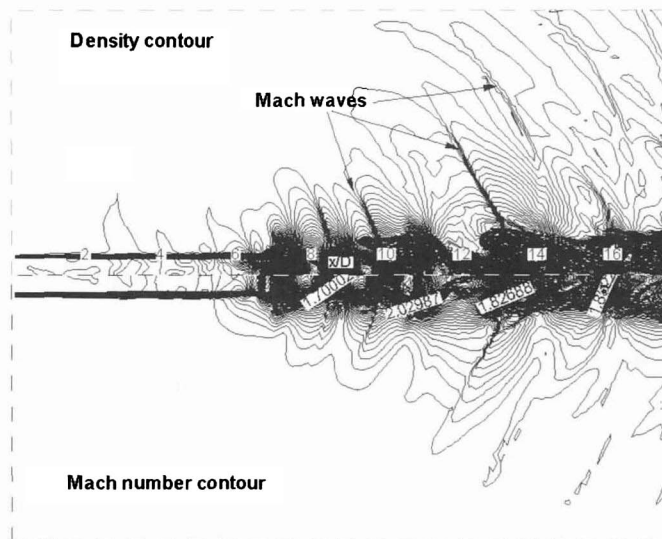

Fig. 6. Instantaneous contours of density and Mach number

Mean flow properties

Fig. 7 shows a distribution of mean Mach number profile on the jet centerline. The present simulations are in fare agreement with experimental data up to near end of potential core. However, a little disagreement is shown at the past of end of potential core because the computations here were restricted to the axisymmric case. At this region, flow transitions are occurred and three-dimensional turbulent effects are known to be quite important. This feature is also shown in radial Mach number profiles of Fig. 8. Radial Mach number profiles show

that the mean flow changes from a profile with a central region of uniform velocity to an approximately Gaussian profile by x/D=10. Near the nozzle exit, the radial profile is nearly perfectly predicted because the present inlet velocity profile was used as a curve fit of experimental data. As going downstream(x/D=5) in the jet shear layer, the discrepancies are increased. While at x/D=10 and 15, fare agreement with experimental data are acquired.
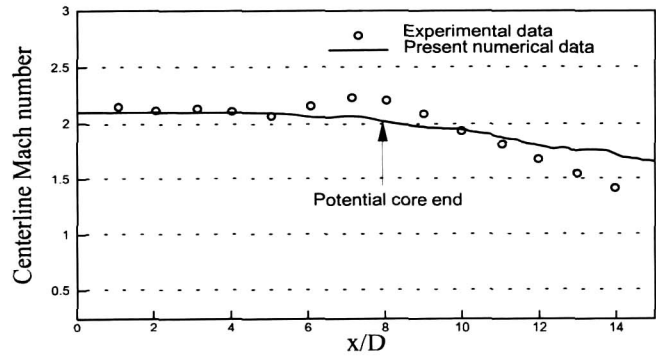

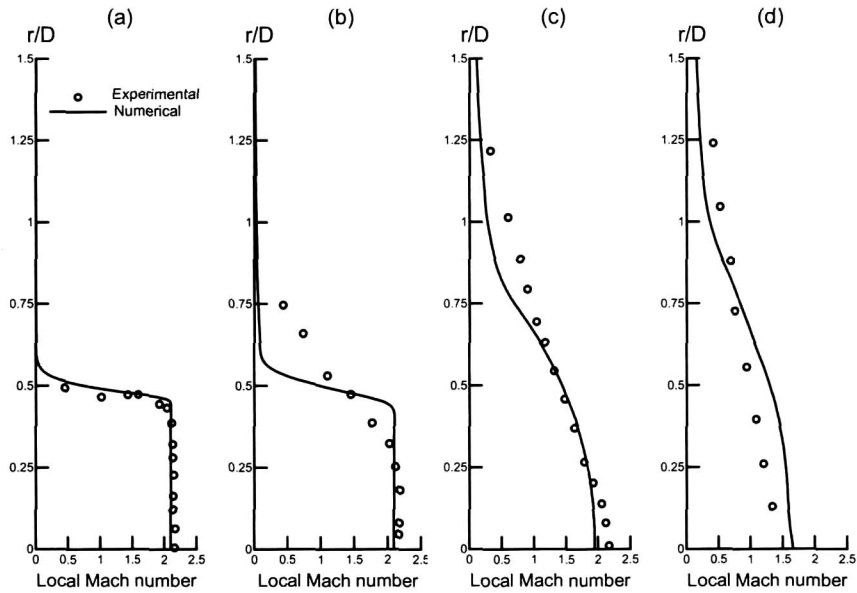Fig. 7. Distribution of mean Mach number on the jet cemterline

Fig. 8. Radial Mach number profiles. x / D : (a) 1 ; (b) 5 ; (c) 10 ; (d) 15

Sound pressure level

Fig. 9 shows overall sound pressure level as a function of the angle from the jet axis. The sound pressure level(SPL) can be obtained as followings

$$SPL = 20\log\left[\frac{\overline{p}'_{rms} p_a}{p_{ref} p_c}\right], \qquad \overline{p}'_{rms} = \sqrt{\lambda \frac{1}{T\to\infty} \frac{1}{T}\int_t^{t+T} p'^2\, dt} \qquad (11)$$

where $\overline{p}'_{rms}$ is the root mean square of the fluctuating sound pressure, p_a is standard atmospheric pressure, p_c is chamber pressure and p_{ref} = 2×10^{-5} N/m^2.

The numerical data and experimental ones are compared at a constant polar radius of 24 jet diameters from the nozzle exit. Experimental result shows that the highest level of generated noise occurs at angle around $30°$ to the jet axis. At this angle, the amplitude of present calculation result is 4~5 dB higher than the experimental one. The reason why the numerical result has serious discrepancy with the experimental one at the angle of $20°$ is that

the present simulation is restricted to the axisymmetric calculation. Therefore, convection velocity of eddies is not decreased by three-dimensional turbulent mixing. At other angles, comparison was given between numerical data and experimental ones with satisfactory results.
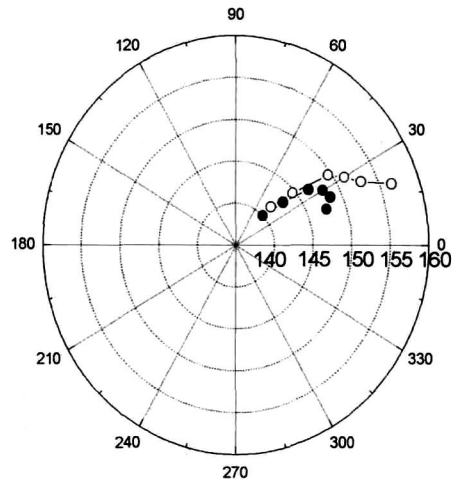

**Fig. 9. Overall sound pressure level directivity ; R/D=24.
O , numerical data; ●, experimental data Unit of
sound pressure level : dB**

Conclusion

In this paper an axisymmetric supersonic jet is simulated at a Mach number 2.1 and a Reynolds number of 70000 to identify the mechanism of Mach wave radiation from the jet. The simulation is based on CAA numerical methods in order to compute directly the aerodynamic noise.

Newly adopted ENO schemes or the nonreflecting boundary conditions showed that an axisymmetric supersonic jet flow could be calculated satisfactorily in the view of mean flow and sound filed..

The mechanism of Mach wave radiation is clearly identified through the pressure and density visualization. Mach waves are generated because large-scale eddies in the jet propagate with a convective velocity, which is supersonic with respect to the surrounding airstream. Aerodynamic properties of the jet, namely meanflow parameters are in fare agreement with experimental data under consideration. However, a little disagreement was shown at the region of end of potential core($x/D \approx 8$). It was found that the three-dimensional effects are important at this region. The experimental result of the sound pressure level shows that the highest level of generated noise occurs at the angle around 30° to the jet axis. At this angle, the amplitude of the present calculation result is 4-5 dB higher than the experimental one. The reason why the numerical result is not in good agreement with experiment seriously at angle around 20° is that the present simulation is restricted to the axisymmetric calculation. So the eddy convection velocity is not decreased by three-dimensional turbulent mixing. At the other angles, the comparison between numerical and experimental data shows the satisfactory results.

References

1. Tam, C. K. W., "Supersonic Jet Noise", *Annu. Rev. Fluid Mech.*, Vol. 27, 1995, pp. 17-43.

2. Tam, C. K. W., and Burton, D.E., "Sound Generated by Instability Waves of Supersonic Flows, Part 2: Axisymmetric jets", *Journal of Fluid Mechanics*, Vol. 138, 1984, pp. 273-295.

3. Tam, C. K. W., and Chen, P., "Turbulent Mixing Noise from Supersonic Jets", *AIAA Journal*, Vol. 32, No. 9, 1994, pp. 1774-1780.

4. J. T. C. Liu, "Developing large-scale wavelike eddies and the near jet noise field", *Journal of Fluid Mechanics*, Vol. 62, 1974, pp. 437-464.

5. D. K. McLaughlin, G. L. Morrison and T. R. Troutt, "Experiments on the instability waves in a supersonic jet and their acoustic radiation", *Journal of Fluid Mechanics*, Vol. 69, 1975, pp. 73-95.

6. G. L. Morrison and D. K. McLaughlin, "Noise Generation by Instabilities in Low Reynolds Number Supersonic Jets", *Journal of Sound and Vibration*, Vol. 65, No. 2, 1979, pp. 177-191.

7. Nakamura, Y. and Yamaguchi, H., "Compressible Jet and Its Sound Emission", *Computational Fluid Dynamics JOURNAL*, Vol. 8, No. 2, 1999, pp. 250-256.

8. M. J. Lighthill, "On sound Generated Aerodynamically, I. General theory", Proceedings of the Royal Society London, Ser. A211, 1952, pp. 564-587.

9. T. R. Troutt and D. K. McLaughlin, "Experiments on the Flow and Acoustic Properties of a Moderate-Reynolds-Number Supersonic Jet", *Journal of Fluid Mechanics*, Vol. 116, 1982, pp. 123-156.

10. Mitchell, B. E., Lele, S. K., and Moin, P., "Direct Computation of Mach Wave Radiation in an Axisymmetric Supersonic Jet", *AIAA Journal*, Vol. 35, No. 10, 1997, pp. 1574-1580.

11. Mitchell, B. E., Lele, S. K., and Moin, P., "Direct Computation of the Sound Generated by Vortex Pairing in an Axisymmetric Jet", *Journal of Fluid Mechanics*, Vol. 383, 1999, pp. 113-142.

12. Freund, J. B., Lele, S.K. and Moin, P., "Direct Simulation Of A Mach 1.92 Jet and Its Sound Field", AIAA/CEAS Paper 98-2291, 1998.

13. Freund, J. B., "Acoustic Sources In A Turbulent Jet : A Direct Numerical Simulation Study", AIAA/CEAS Paper 99-1858, 1999.

14. R. R. Mankbadi, M. E. Hayer, and L. A. Povinelli, "Structure of Supersonic Jet Flow and Its Radiated Sound", *AIAA Journal*, Vol. 32, No. 5, 1994, pp. 897-906.

15. C. Bogey, C. Bailly and D. Juve, "Computation of the Sound Radiated by a 3-D Jet Using Large Eddy Simulation", AIAA Paper 2000-2009, June 2000.

16. W. Zhao, S. H. Frankel and L. Mongeau, "Large Eddy Simulation of Sound Radiation from a Subsonic Turbulent Jet," AIAA Paper 2000-2078, June 2000.

17. Hoffmann, K. A., "Computational Fluid Dynamics for Engineers", *Engineering Education System*, Vol. 2, pp. 25-28.

18. Harten, A., "High Resolution Schemes for Hyperbolic Conservation Laws", Journal of Computational Physics, Vol. 49, No. 3. 1983, pp. 357-393.

19. Kim, Y. S. and Lee, D. J., "Numerical Analysis of Internal Combustion Engine Intake Noise with a Moving piston and a Valve", *Journal of Sound and Vibration*, Vol. 241, No. 5, 2001, pp. 895-912.

20. Kim, Y. S., and D. J. Lee, "Computation of Shock-Sound Interaction Using Finite Volume Essentially Nonoscillatory Scheme", *AIAA Journal*, Vol. 40, No 6, 2002, pp.1239-1240.

21. C. K. W. Tam, "Advances in Numerical Boundary Conditions for Computational Aeroacoustics", *AIAA Paper 97-1774*, 1997, pp. 1-16.

22. Thompson, K. W., "Time Dependent Boundary Conditions for Hyperbolic Systems", *Journal of Computational Physics,* Vol. 68, 1987, pp.1-24.

23. Thompson, K. W., "Time Dependent Boundary Conditions for Hyperbolic Systems II", *Journal of Computational Physics,* Vol. 89, 1990, pp. 439-461.

24. Poinsot, T. J. and Lele, S. K., "Boundary Conditions for Direct Simulations of Compressible Viscous Flow", *Journal of Computational Physics,* Vol. 101, 1992, pp. 104-129.